LETTER

doi:10.1038/nature11059

Astrocyte glypicans 4 and 6 promote formation of excitatory synapses via GluA1 AMPA receptors

Nicola J. Allen[1]†, Mariko L. Bennett[1], Lynette C. Foo[1], Gordon X. Wang[2], Chandrani Chakraborty[1], Stephen J. Smith[2] & Ben A. Barres[1]

In the developing central nervous system (CNS), the control of synapse number and function is critical to the formation of neural circuits. We previously demonstrated that astrocyte-secreted factors powerfully induce the formation of functional excitatory synapses between CNS neurons[1]. Astrocyte-secreted thrombospondins induce the formation of structural synapses, but these synapses are postsynaptically silent[2]. Here we use biochemical fractionation of astrocyte-conditioned medium to identify glypican 4 (Gpc4) and glypican 6 (Gpc6) as astrocyte-secreted signals sufficient to induce functional synapses between purified retinal ganglion cell neurons, and show that depletion of these molecules from astrocyte-conditioned medium significantly reduces its ability to induce postsynaptic activity. Application of Gpc4 to purified neurons is sufficient to increase the frequency and amplitude of glutamatergic synaptic events. This is achieved by increasing the surface level and clustering, but not overall cellular protein level, of the GluA1 subunit of the AMPA (α-amino-3-hydroxy-5-methyl-4-isoxazole propionic acid) glutamate receptor (AMPAR). Gpc4 and Gpc6 are expressed by astrocytes *in vivo* in the developing CNS, with Gpc4 expression enriched in the hippocampus and Gpc6 enriched in the cerebellum. Finally, we demonstrate that Gpc4-deficient mice have defective synapse formation, with decreased amplitude of excitatory synaptic currents in the developing hippocampus and reduced recruitment of AMPARs to synapses. These data identify glypicans as a family of novel astrocyte-derived molecules that are necessary and sufficient to promote glutamate receptor clustering and receptivity and to induce the formation of postsynaptically functioning CNS synapses.

To understand how astrocytes regulate functional synapse formation, we examined postsynaptic function, AMPAR levels and AMPAR localization at synapses between purified retinal ganglion cells (RGCs) cultured alone or with a feeder layer of astrocytes (Supplementary Fig. 1a–d). Astrocytes strengthen individual excitatory glutamatergic synapses in RGCs, as shown by increased frequency and amplitude of miniature excitatory postsynaptic currents[1] (mEPSCs) (Fig. 1a–c). In RGCs, mEPSCs are mediated purely by AMPARs, composed of combinations of four subunits, GluA1 to GluA4, forming tetramers[1,3]. Astrocytes do not greatly alter total AMPAR levels in RGCs (except for a small significant increase in GluA4), and thus do not induce the synthesis of new AMPARs or block the degradation of existing receptors (Fig. 1d, e). Astrocytes do, however, increase surface levels of all AMPAR subunits on RGCs by a factor of three, as shown by surface biotinylation and quantitative western blotting (Fig. 1f, g). Surface staining for GluA1-containing AMPARs demonstrated that the increased surface receptors are clustered together in puncta throughout the dendrites (Fig. 1h–j). These results demonstrate that astrocyte-derived signals lead to increased surface levels and clustering of pre-existing AMPARs.

We previously identified thrombospondins and hevin as astrocyte-secreted proteins sufficient to induce structural synapse formation, but the synapses so formed are postsynaptically silent because they lack AMPARs[2,4]. Therefore, we used biochemistry to identify the astrocyte-secreted factor that is sufficient to induce functional synapse formation. Astrocytes were maintained in minimal medium and the factors they secreted collected as astrocyte-conditioned medium (ACM), which was concentrated and fed to RGCs, and was sufficient to induce functional synapse formation as assessed by electrophysiological recording of total synaptic activity and mEPSCs (Supplementary Fig. 1c, e–g). Analysis of ACM by two-dimensional electrophoresis revealed that hundreds of proteins were present, and size-exclusion experiments demonstrated the activity factor to be relatively large, between 100 and 300 kDa (Supplementary Fig. 2). To narrow down candidate factors present in ACM, we conducted affinity column fractionation, initially using individual columns and then combining them in series (Supplementary Fig. 3). In the final fractionation scheme, the unbound proteins were taken from a heparin column, bound and eluted from an anion column, and then bound and eluted from a hydrophobic interaction column. This final eluted protein fraction was fed to RGCs, and as it was unclear whether the activity factor would be sufficient to induce synapses directly, thrombospondin was included to induce structural synapse formation. This final fraction was sufficient to induce a large increase in synaptic activity (Fig. 1k), contained 1% of the starting protein (Supplementary Table 1) and was sixfold enriched for functional activity. This fraction was analysed by mass spectrometry and contained approximately 25 candidate factors (Supplementary Table 2).

To identify which candidate protein was sufficient to enhance synaptic activity, we overexpressed them in COS-7 cells (which do not secrete endogenous synaptogenic factors (Supplementary Fig. 4)) and fed the conditioned medium to RGCs along with thrombospondin. Most of the candidates lacked activity, whereas medium conditioned by Gpc4-expressing COS-7 cells was sufficient to induce a large increase in synaptic activity (Supplementary Fig. 4 and Fig. 1l). Western blotting of conditioned media from RGCs, cultured astrocytes and immunopanned astrocytes (that closely resemble *in vivo* mature astrocytes[5]) demonstrated that astrocytes and not neurons secrete Gpc4 *in vitro* (Supplementary Fig. 5). Glypicans are a conserved family of heparan sulphate proteoglycans, with six members (Gpc1 to Gpc6) in mammals, and Gpc4 is homologous to *Drosophila* Dally-like[6]. The 63-kDa core protein is heavily glycosylated and can be in excess of 200 kDa in mass. Glypicans are tethered to the extracellular face of the plasma membrane of cells by GPI (glycosyl phosphoinositide) linkages[7,8], which can be cleaved by endogenous phospholipases, thus releasing the protein.

Having demonstrated that Gpc4 is sufficient to enhance total synaptic activity, we asked whether this was due to effects on postsynaptic strengthening of synapses. In subsequent experiments, RGCs were treated with purified Gpc4 (Supplementary Fig. 6a, b), in the absence of thrombospondin, to assess specific effects of Gpc4 on synapse formation and function. Gpc4 was sufficient to strengthen individual

[1]Stanford University School of Medicine, Department of Neurobiology, 299 Campus Drive, Fairchild Science Building D231, Stanford, California 94305-5125, USA. [2]Stanford University School of Medicine, Department of Molecular and Cellular Physiology, 279 Campus Drive, Beckman Center B100, Stanford, California 94305-5125, USA. †Present address: Molecular Neurobiology Laboratory, The Salk Institute for Biological Studies, 10010 North Torrey Pines Road, La Jolla, California 92037, USA.

©2012 Macmillan Publishers Limited. All rights reserved

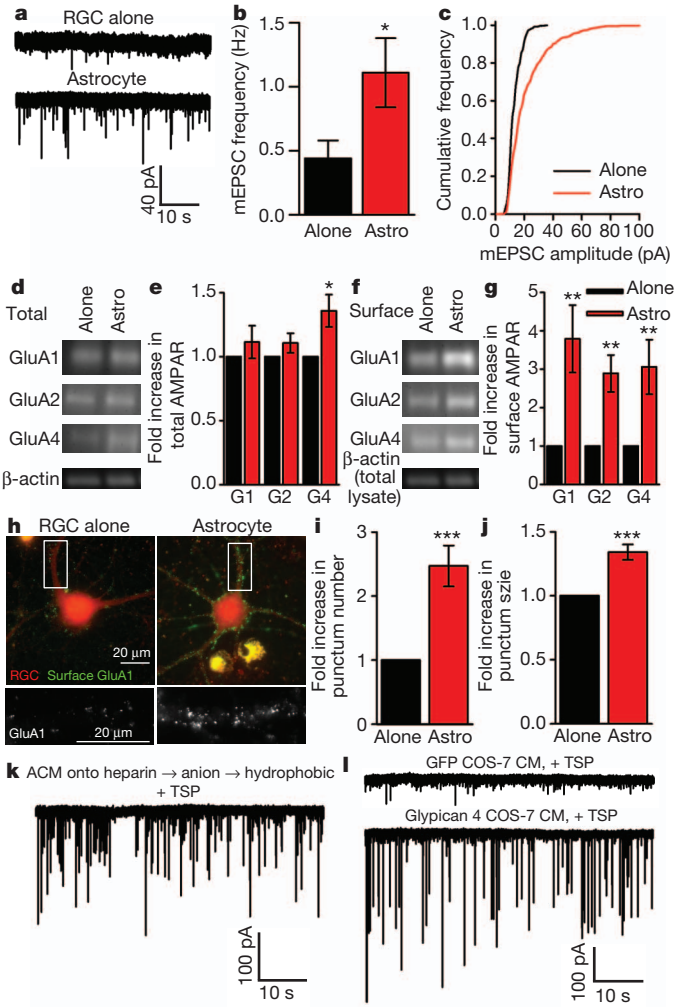

Figure 1 | Astrocyte signals strengthen synapses by recruitment of surface AMPARs. **a**–**c**, Example mEPSC recordings (**a**) show that frequency (**b**) and amplitude (**c**) are significantly increased in RGCs cultured with astrocytes. Average mEPSC amplitude: 12.2 ± 0.5 pA (RGCs alone, $N = 13$ cells), 20.4 ± 1.7 pA (astrocytes, $N = 14$, $P < 0.0002$). **d**, **e**, Astrocytes do not alter total AMPAR levels in RGCs. Western blots (**d**) of RGC lysates for AMPAR subunits GluA1 (G1), GluA2 (G2) and GluA4 (G4), and β-actin loading control, and quantification of band intensity relative to RGC alone (**e**). $N = 7$ experiments. **f**, **g**, Astrocytes increase surface AMPARs in RGCs. Western blots (**f**) of surface AMPAR subunits GluA1, GluA2 and GluA4, and β-actin loading control from total lysate (same experiment as **d**), and quantification of band intensity relative to RGC alone (**g**). $N = 16$ experiments. **h**–**j**, Astrocytes cluster GluA1-containing AMPARs on the RGC surface. Example images (**h**) of surface GluA1 (green) and RGC processes (red); bottom panel, enlargement of GluA1 (boxed white). Quantification of number (**i**) and size (**j**) of GluA1 clusters. $N = 10$ experiments. **k**, Total synaptic activity induced by final protein fraction from column fractionation of ACM. **l**, Total synaptic activity in RGCs cultured in COS-7-cell-conditioned medium (COS-7 CM) transfected with a control protein (green fluorescent protein (GFP)) or Gpc4, plus thrombospondin (TSP). $^*P < 0.05$, $^{**}P < 0.01$, $^{***}P < 0.001$; error bars, s.e.m.

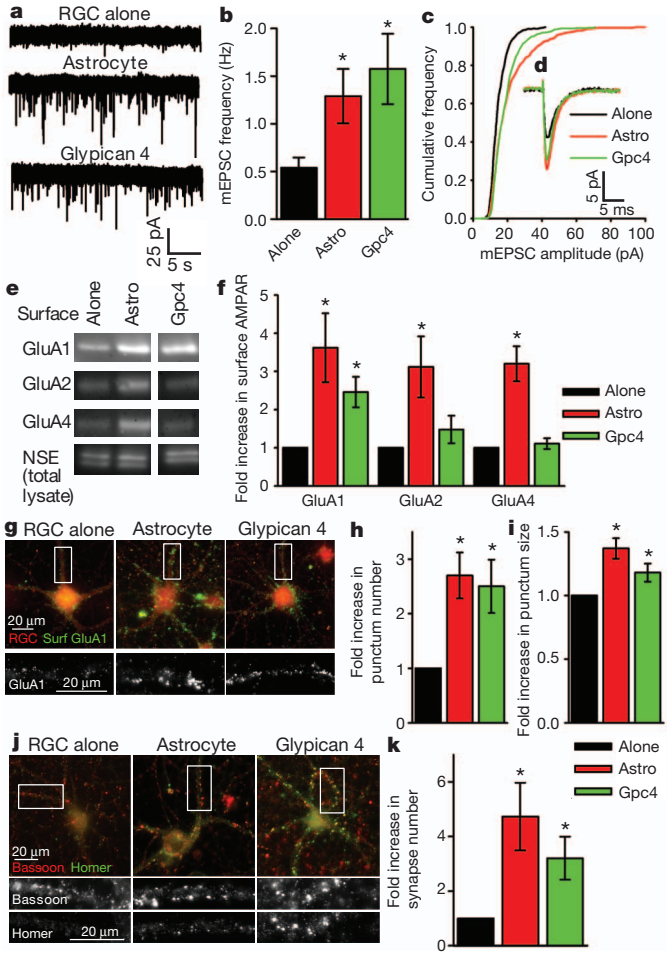

Figure 2 | Gpc4 is sufficient to strengthen glutamatergic synapses and increase surface GluA1-containing AMPARs. **a**–**d**, Example mEPSC recordings (**a**) show that frequency (**b**) and amplitude (**c**) are significantly increased in RGCs cultured with Gpc4. Average traces aligned by rise time (**d**). Average mEPSC amplitude: 13.8 ± 0.7 pA (RGC alone, $N = 16$ cells), 20.0 ± 1.2 pA (astrocyte, $N = 16$, $P < 0.05$), 17.8 ± 1.4 pA (Gpc4, $N = 13$, $P < 0.05$). **e**, **f**, Gpc4 increases surface GluA1 AMPARs in RGCs. Western blots (**e**) of surface AMPAR subunits GluA1, GluA2 and GluA4 and neuron-specific enolase (NSE) loading control from total lysate, and quantification of band intensity relative to RGC alone (**f**). For full blot results, see Supplementary Fig. 9. $N = 6$ experiments for GluA1 and GluA2; $N = 3$ for GluA4. **g**–**i**, Gpc4 clusters GluA1-containing AMPARs on the RGC surface. Example images (**g**) of surface GluA1 (green) and RGC processes (red); bottom panel, enlargement of GluA1 (boxed white). Quantification of number (**h**) and size (**i**) of GluA1 clusters. $N = 7$ experiments. **j**, **k**, Gpc4 induces structural synapses. Example images (**j**) of presynaptic (bassoon, red) and postsynaptic (homer, green) staining; bottom panels, enlargements of the respective markers (boxed white). Quantification of synapse number (**k**) (co-localization of pre- and postsynaptic puncta). $N = 6$ experiments. $^*P < 0.05$; error bars, s.e.m.

synapses, as shown by increased mEPSC frequency and amplitude, although the very large-amplitude events induced by astrocytes were absent (Fig. 2a–d and Supplementary Fig. 7). To determine whether increased synaptic activity was due to increased numbers of AMPARs on the cell surface, we isolated surface receptors and analysed them by western blotting. Gpc4 induced a 2.5-fold increase in surface GluA1, comparable to that observed in the presence of astrocytes; however, there was less of an increase in surface levels of the other subunits (Fig. 2e, f and Supplementary Fig. 9). Thus, Gpc4 specifically recruits GluA1-containing AMPARs, and astrocytes release additional factors that bring GluA2, GluA3 and GluA4 AMPAR subunits to the synapse. Surface staining for GluA1 revealed a 2.5-fold increase in the number of receptor clusters on RGCs exposed to Gpc4, and a 20% increase in size, comparable to astrocytes (Fig. 2g–i). Gpc4-induced clustering of GluA1 on RGCs is dose dependent, being effective at 0.1–10 nM (comparable to levels in ACM) and ineffective at higher concentrations (Supplementary Fig. 6c, d). These experiments demonstrate that Gpc4 is sufficient to strengthen pre-existing synapses by increasing mEPSC amplitude; however, we also observed an increase in the number of mEPSCs and GluA1 clusters on RGCs, suggesting that Gpc4 can induce new structural synapses. We assessed synapse number by counting co-localization of pre- and postsynaptic markers, and observed a significant threefold increase in synapse number in RGCs treated with Gpc4

©2012 Macmillan Publishers Limited. All rights reserved

compared with RGCs grown alone (Fig. 2j, k). This demonstrates that Gpc4 is synaptogenic, although to a lesser degree than astrocytes.

The glypicans are a gene family with six members in mouse and human; *Gpc6* is the most homologous to *Gpc4* (ref. 9). We identified both Gpc4 and Gpc6 in the fractionation positive fraction (Supplementary Table 2), so we assessed whether Gpc6 is also synaptogenic. Gpc6 was sufficient to recruit GluA1 to the neuronal surface, and also induced structural synapse formation to the same extent as Gpc4 (Supplementary Fig. 8). To determine whether Gpc4 and Gpc6 are necessary for ACM to enhance postsynaptic activity, we used short interfering RNA (siRNA) to reduce expression of both in astrocytes, and confirmed protein reduction in ACM by western blotting (Supplementary Fig. 10a). ACM with reduced Gpc4 and Gpc6 was unable to significantly increase mEPSC amplitude in RGCs (Fig. 3a–c) and unable to cluster GluA1 on the neuronal surface (Fig. 3d and Supplementary Fig. 10c, d). Overexpression of the human form of Gpc4, which is resistant to the siRNA, rescued the ability of ACM to cluster GluA1 receptors on the neuronal surface (Fig. 3d). The use of siRNA against individual glypicans was not as effective in reducing the ability of ACM to enhance total synaptic activity (Supplementary Fig. 10b). ACM with reduced levels of Gpc4 and Gpc6 still induced a significant increase in structural synapse formation, presumably owing to the presence of other synaptogenic proteins such as thrombospondin and hevin[2,4] (Fig. 3e). These results show that Gpc4 and Gpc6 are necessary components of ACM for enhancing postsynaptic activity, and that there is functional redundancy between family members.

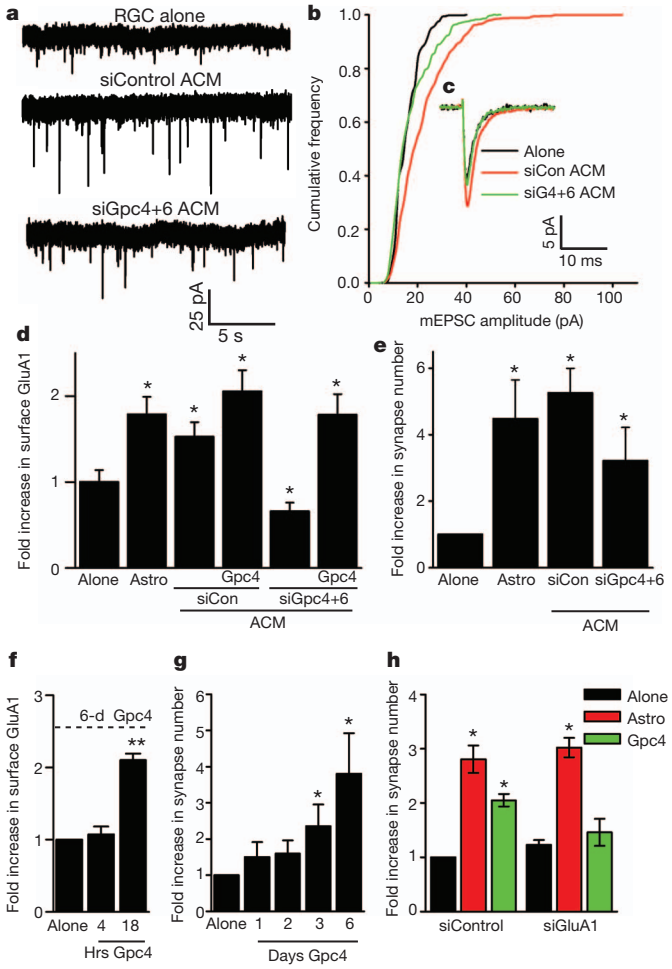

Figure 3 | Gpc4 and Gpc6 are necessary for ACM to cluster surface GluA1, and mechanism of action. **a**–**c**, Reduction of Gpc4 and Gpc6 levels in ACM reduces its ability to increase mEPSC amplitude in RGCs. Example mEPSC recordings (**a**), cumulative amplitude plot (**b**) and average traces aligned by rise time (**c**). Average mEPSC amplitude: 14.6 ± 0.6 pA (RGC alone, $N = 8$ cells), 20.6 ± 0.9 pA (siRNA control ACM, $N = 10$, $P < 0.05$), 16.0 ± 1.0 pA (siRNA Gpc4 and Gpc6 ACM, $N = 11$, $P = 0.3$). **d**, Reduction of Gpc4 and Gpc6 levels in ACM prevents GluA1 surface clustering, which is rescued by expression of siRNA-resistant Gpc4. $N = 30$ cells per condition. **e**, Reduction of Gpc4 and Gpc6 levels in ACM does not prevent ACM-induced structural synapse formation. $N = 3$ experiments. **f**, Time course of Gpc4-induced surface clustering of GluA1 shows 18 h of treatment is required to increase surface GluA1 levels. Dashed line, 6-d data from Fig. 2h. $N = 3$ experiments (4 h), 4 (18 h). **g**, Gpc4 does not rapidly induce structural synapse formation and requires 3 d of treatment. $N = 5$ experiments (1 d), 3 (2 d), 6 (3 d), 3 (6 d). **h**, Surface clustering of GluA1 is necessary for Gpc4-induced synapse formation, shown by the inability of Gpc4 to induce synapse formation in RGCs lacking GluA1. $N = 5$ experiments. $^*P < 0.05$, $^{**}P < 0.0001$; error bars, s.e.m.

To examine the time course of Gpc4 effects, we assayed surface clustering of GluA1 after 4 h and 18 h of treatment. There was no increase in receptor recruitment after 4 h, but after 18 h there was a significant increase in surface GluA1, to the same level as after 6 d (time point previously used; Fig. 3f and Supplementary Fig. 11a, b). Thus, Gpc4 does not immediately capture GluA1 AMPARs on the surface of the cell, which suggests that downstream signalling cascades are involved. We examined structural synapse formation at 4 h, 18 h, 1 d, 2 d, 3 d and 6 d after Gpc4 addition, and found that synapse number only significantly increased after 3 d (Fig. 3g and Supplementary Fig. 11c, d). Therefore, Gpc4 first clusters GluA1-containing AMPARs on the cell surface, and only then recruits postsynaptic scaffolding molecules. This suggests that clustering of GluA1 is a necessary step in Gpc4-induced synapse formation. To test this hypothesis, we used siRNA to decrease GluA1 in RGCs, and asked whether Gpc4 could still induce structural synapse formation (Supplementary Fig. 11e). Whereas astrocytes still increased synapse formation in RGCs lacking GluA1, Gpc4 did not (Fig. 3h). This mechanism of synaptogenesis is distinct from that of thrombospondin, which induces structural synapses that are postsynaptically silent[2]. Thus, astrocytes can induce excitatory synapse formation by at least two distinct mechanisms (Supplementary Fig. 19).

Because they are heparan sulphate proteoglycans, glypicans can interact with signalling receptors and morphogens (for example Wnt, fibroblast growth factor, Hedgehog and bone morphogenetic protein) via their sugar chains[10]. We generated a 'mutant' form of Gpc4 lacking glycosylation sites to investigate whether glycosylation is necessary for the synaptogenic effects of Gpc4 (Supplementary Fig. 12a). Glycosylation-deficient Gpc4 could not cluster GluA1 or induce structural synapse formation (Supplementary Fig. 12b, c and Supplementary Fig. 6d). Comparison by mass spectrometry of co-purified factors between full and mutant Gpc4 produced by HEK cells showed few differences between them, and these factors were not detected when Gpc4 was purified from astrocytes (data not shown), which can induce an increase in synaptic activity (Fig. 2a–d). We nevertheless tested a number of known glypican interactors for their ability to cluster surface GluA1 on RGCs and found none to be effective (Supplementary Fig. 12d). Thus, modification of Gpc4 by heparan sulphate is necessary for its synaptogenic activity, and this may be due to the necessity of heparan sulphate for structural interaction with a receptor rather than delivery of associated morphogens, as has been shown for Dally-like binding to its receptor LAR[11].

We next investigated the roles of Gpc4 and Gpc6 in developmental synapse formation and maturation *in vivo*. *In situ* hybridization revealed overlapping messenger RNA expression throughout the brain during postnatal development, particularly in the cortex, with Gpc4 enriched in the hippocampus and Gpc6 enriched in the cerebellum (Fig. 4a and Supplementary Fig. 13a). Prior gene profiling of purified forebrain CNS cells showed that messenger RNA for both Gpc4 and Gpc6 is highly enriched in astrocytes compared with neurons[12] (Supplementary Fig. 14a), which we confirmed using quantitative real-time PCR of purified astrocytes and neurons from the cortex and hippocampus (Supplementary Fig. 14b, c). Combining *in situ*

©2012 Macmillan Publishers Limited. All rights reserved

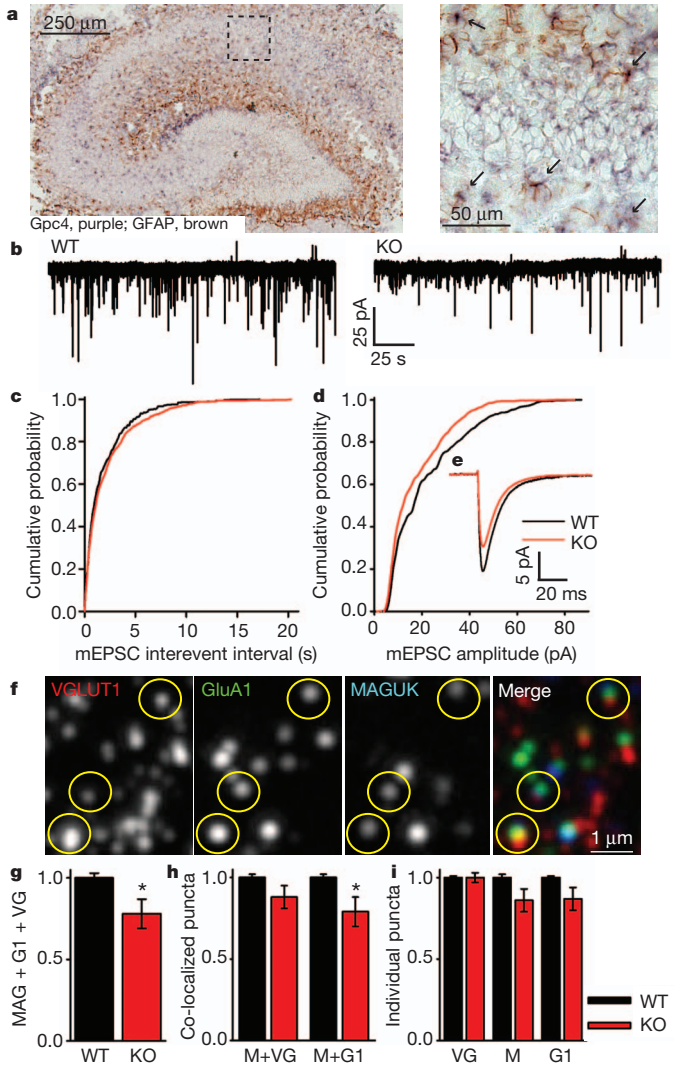

Figure 4 | Mice deficient in Gpc4 have weaker excitatory synapses *in vivo*. **a**, *In situ* hybridization of Gpc4 messenger RNA in P6 mouse hippocampus. Left: Gpc4 (purple) is expressed in synaptic regions and co-localizes with astrocytes (glial fibrillary acidic protein (GFAP), brown). Right: enlargement of boxed region; arrows mark Gpc4-positive astrocytes. **b**–**e**, Mice lacking Gpc4 (KO) have weaker excitatory synapses in CA1 pyramidal neurons at P12. Example mEPSC recordings (**b**), cumulative probability plot of mEPSC interevent interval (**c**) (no significant difference in frequency: wild type, 0.88 ± 0.25 Hz; *Gpc4*-knockout, 0.55 ± 0.08 Hz; $P = 0.16$), cumulative probability plot of mEPSC amplitude (**d**) (significant decrease in amplitude: wild type, 20.67 ± 2.16 pA; *Gpc4*-knockout, 16.07 ± 0.96 pA; $P < 0.05$), average traces aligned by rise time (**e**). $N = 9$ cells (*Gpc4*-knockout, five mice), 6 (wild type, five mice). **f**–**i**, Mice lacking Gpc4 recruit fewer GluA1 AMPARs to synaptic sites in hippocampal CA1 at P12. Example array tomography image (**f**) from wild type; VGLUT1 (red), GluA1 (green), MAGUK (blue), triple co-localization (yellow circles). There is a significant decrease in triple co-localization of VGLUT1 + MAGUK + GluA1 in *Gpc4*-knockout mice (**g**). There is no significant difference in structural synapse number (VGLUT1 + MAGUK), but there is a significant decrease in GluA1 association with MAGUK in *Gpc4*-knockout mice (**h**) and no difference in individual synaptic markers (**i**). $N = 10$ arrays per genotype from four wild-type and four *Gpc4*-knockout mice. *$P < 0.05$; error bars, s.e.m.

hybridization for Gpc4 with immunostaining for the astrocyte marker GFAP demonstrated that hippocampal astrocytes express Gpc4 at early postnatal periods (P6–P14) during the initiation of synaptogenesis[13], and that astrocytic expression decreases with maturation (P21) and switches to subsets of neurons (Fig. 4a and Supplementary Fig. 13b–d). Therefore, developing astrocytes express different glypicans with distinct but overlapping regional patterns.

To determine the *in vivo* function of Gpc4, we examined synapse formation and function in hippocampal area CA1 of *Gpc4*-knockout mice, and chose this region because Gpc4 is enriched here (Supplementary Fig. 13a) and Gpc4 and Gpc6 have redundant functions *in vitro*. We recorded mEPSCs from CA1 pyramidal neurons in acute hippocampal slices from *Gpc4*-knockout and wild-type littermate controls at P12, during functional synapse formation, and at P24, when more mature synapses are present. We observed a significant (22%) decrease in the amplitude of mEPSCs at P12, and at P24 a significant shift in amplitude distribution remained (Fig. 4b–e and Supplementary Figs 15 and 16). These effects were not due to gross differences in dendritic architecture or neuronal membrane properties (Supplementary Fig. 17), or to changes in total levels of synaptic proteins (Supplementary Fig. 18). We used array tomography to address whether the decreased mEPSC amplitude was due to a defect in structural synapse formation or to reduced recruitment of GluA1 receptors to synapses in hippocampal area CA1. Functional excitatory synapses were classified by triple co-localization of the presynaptic vesicular marker VGLUT1 with the postsynaptic density marker MAGUK, plus GluA1 at the postsynaptic side (Fig. 4f). There is a significant (22%) decrease in this class of synapse at P12 in *Gpc4*-knockout mice (Fig. 4g). This decrease is not due to a difference in the number of individual puncta (Fig. 4i) or to less structural synapse formation (VGLUT1 + MAGUK is not altered), but to a significant decrease in the co-localization of GluA1 with MAGUK (Fig. 4h). Therefore, the same number of synapses form in *Gpc4*-knockout mice as in wild type, but these synapses recruit fewer GluA1 AMPARs, probably leading to the observed physiological defect of smaller mEPSCs. The amplitude decrease observed is similar to that seen when the GluA1 subunit of the AMPAR is removed from CA1 pyramidal neurons[14,15], and this is the subunit we have shown to be recruited to the surfaces of RGCs by Gpc4 *in vitro* (Fig. 2e, f).

Here we have identified glypicans as a novel family of astrocyte-secreted proteins that regulate glutamate receptor clustering and excitatory synapse formation in neurons. Other secreted factors have been described that can induce structural synapses that are post-synaptically silent (thrombospondins and hevin[2,4]), increase surface AMPAR levels (neuronal pentraxins and tumour necrosis factor-α (refs 16, 17)) or alter AMPAR mobility and synaptic plasticity (extracellular matrix molecules[18]). Glypicans are the first non-neuronal secreted factors to be identified that are sufficient to induce functional synapses that cluster pre- and postsynaptic density proteins, are postsynaptically active and contain surface AMPARs. We have demonstrated that astrocytes increase GluA1 to GluA4 on the surfaces of neurons and that Gpc4 and Gpc6 specifically regulate GluA1 surface expression, indicating that astrocytes produce multiple factors that regulate the surface expression of different AMPAR subunits. Notably, specific AMPAR subunits may be used for the developmental initiation of synapse formation and also for the strengthening of synapses during long-term potentiation, with GluA1 used during synapse initiation and GluA2 and GluA3 used during synapse maturation[19–22]. This would be consistent with a role for glypicans in initiating nascent synapse formation by recruiting postsynaptic GluA1, followed by the action of additional factors that induce synapse maturation. Astrocytes may control these events by releasing distinct factors, including glypicans and thrombospondin, with spatiotemporal specificity, providing a new mechanism by which astrocytes control the formation and maturation of neural circuitry.

An attractive candidate receptor for inducing the actions of Gpc4 and Gpc6 is LAR, a protein tyrosine phosphatase receptor. *Drosophila* Dally-like can bind to and signal through LAR[11], and removal of LAR family members from mammalian hippocampal neurons reduces their ability to form synapses and to recruit AMPARs to synapses[23]. Mice lacking Gpc6 die shortly after birth[24] from apparent breathing difficulties (N.J.A. and B.A.B., unpublished observations), suggesting neural dysfunction, which is reminiscent of the phenotype observed in

©2012 Macmillan Publishers Limited. All rights reserved

neuroligin-triple-knockout mice[25]. In addition, mutations in Gpc6 have been associated with attention deficit hyperactivity disorder[26] and neuroticism[27] in humans, disorders in which synaptic dysfunction has been implicated. Thus, the identification of glypicans as regulators of functional synapse formation has important implications for the formation of appropriate neuronal circuits in development and disease.

METHODS SUMMARY

For detailed methods, see Methods.

Purification and culture of RGCs and astrocytes. RGCs were purified by sequential immunopanning to greater than 99% purity from P5–P7 Sprague-Dawley rats (Charles Rivers) and cultured in serum-free medium containing BDNF, CNTF and forskolin on laminin-coated coverslips at 50,000 cells per well, as previously described[1,2]. Cortical astrocytes (MD astrocytes) were prepared as described in ref. 1. RGCs were cultured for 7–10 d to allow robust process outgrowth, and were then cultured with astrocyte inserts, ACM, COS-7-conditioned media, thrombospondin, Gpc4 or Gpc6 for an additional 6 d unless stated otherwise.

Column fractionation procedure. ACM (3.3 mg), collected from 10×15 cm plates of astrocytes, was diluted in ethanolamine buffer and passed over a heparin column to which the protein of interest did not bind. The unbound fraction was collected and passed over an anion column (Q column), to which the protein of interest did bind. The NaCl (salt) concentration was increased to 0.5 M to remove irrelevant proteins, and then to 2 M to elute proteins of interest. The 0.5–2 M anion column eluate was passed over a hydrophobic interaction column (phenyl (low sub)), to which the protein of interest did bind. The bound proteins were eluted by decreasing the NaCl concentration from 2 M to 0 M. This final eluate contained 32 μg protein (Supplementary Table 1) and was sixfold enriched for functional activity, and was analysed by mass spectrometry.

Mice. *Gpc4*-knockout mice were obtained from Genentech/Lexicon and were generated by homologous recombination targeting exon 3, confirmed by Southern blotting[24]. No Gpc4 was detected by western-blotting-conditioned media prepared from *Gpc4*-knockout astrocytes, demonstrating that no functional protein was being secreted (Supplementary Fig. 5c).

Full Methods and any associated references are available in the online version of the paper at www.nature.com/nature.

Received 15 December 2010; accepted 16 March 2012.

Published online 27 May 2012.

1. Ullian, E. M., Sapperstein, S. K., Christopherson, K. S. & Barres, B. A. Control of synapse number by glia. *Science* **291,** 657–661 (2001).
2. Christopherson, K. S. *et al.* Thrombospondins are astrocyte-secreted proteins that promote CNS synaptogenesis. *Cell* **120,** 421–433 (2005).
3. Traynelis, S. F. *et al.* Glutamate receptor ion channels: structure, regulation, and function. *Pharmacol. Rev.* **62,** 405–496 (2010).
4. Kucukdereli, H. *et al.* Control of excitatory CNS synaptogenesis by astrocyte-secreted proteins Hevin and SPARC. *Proc. Natl Acad. Sci. USA* **108,** E440–E449 (2011).
5. Foo, L. C. *et al.* Development of a method for the purification and culture of rodent astrocytes. *Neuron* **71,** 799–811 (2011).
6. Ybot-Gonzalez, P., Copp, A. J. & Greene, N. D. Expression pattern of glypican-4 suggests multiple roles during mouse development. *Dev. Dyn.* **233,** 1013–1017 (2005).
7. Song, H. H. & Filmus, J. The role of glypicans in mammalian development. *Biochim. Biophys. Acta* **1573,** 241–246 (2002).
8. Watanabe, K., Yamada, H. & Yamaguchi, Y. K-glypican: a novel GPI-anchored heparan sulfate proteoglycan that is highly expressed in developing brain and kidney. *J. Cell Biol.* **130,** 1207–1218 (1995).
9. De Cat, B. & David, G. Developmental roles of the glypicans. *Semin. Cell Dev. Biol.* **12,** 117–125 (2001).
10. Van Vactor, D., Wall, D. P. & Johnson, K. G. Heparan sulfate proteoglycans and the emergence of neuronal connectivity. *Curr. Opin. Neurobiol.* **16,** 40–51 (2006).
11. Johnson, K. G. *et al.* The HSPGs Syndecan and Dally-like bind the receptor phosphatase LAR and exert distinct effects on synaptic development. *Neuron* **49,** 517–531 (2006).
12. Cahoy, J. D. *et al.* A transcriptome database for astrocytes, neurons, and oligodendrocytes: a new resource for understanding brain development and function. *J. Neurosci.* **28,** 264–278 (2008).
13. Hsia, A. Y., Malenka, R. C. & Nicoll, R. A. Development of excitatory circuitry in the hippocampus. *J. Neurophysiol.* **79,** 2013–2024 (1998).
14. Lu, W. *et al.* Subunit composition of synaptic AMPA receptors revealed by a single-cell genetic approach. *Neuron* **62,** 254–268 (2009).
15. Andrasfalvy, B. K., Smith, M. A., Borchardt, T., Sprengel, R. & Magee, J. C. Impaired regulation of synaptic strength in hippocampal neurons from GluR1-deficient mice. *J. Physiol. (Lond.)* **552,** 35–45 (2003).
16. O'Brien, R. J. *et al.* Synaptic clustering of AMPA receptors by the extracellular immediate-early gene product Narp. *Neuron* **23,** 309–323 (1999).
17. Beattie, E. C. *et al.* Control of synaptic strength by glial TNF-α. *Science* **295,** 2282–2285 (2002).
18. Frischknecht, R. *et al.* Brain extracellular matrix affects AMPA receptor lateral mobility and short-term synaptic plasticity. *Nature Neurosci.* **12,** 897–904 (2009).
19. Kumar, S. S., Bacci, A., Kharazia, V. & Huguenard, J. R. A developmental switch of AMPA receptor subunits in neocortical pyramidal neurons. *J. Neurosci.* **22,** 3005–3015 (2002).
20. Friedman, H. V., Bresler, T., Garner, C. C. & Ziv, N. E. Assembly of new individual excitatory synapses: time course and temporal order of synaptic molecule recruitment. *Neuron* **27,** 57–69 (2000).
21. Groc, L., Gustafsson, B. & Hanse, E. AMPA signalling in nascent glutamatergic synapses: there and not there! *Trends Neurosci.* **29,** 132–139 (2006).
22. Malinow, R. & Malenka, R. C. AMPA receptor trafficking and synaptic plasticity. *Annu. Rev. Neurosci.* **25,** 103–126 (2002).
23. Dunah, A. W. *et al.* LAR receptor protein tyrosine phosphatases in the development and maintenance of excitatory synapses. *Nature Neurosci.* **8,** 458–467 (2005).
24. Tang, T. *et al.* A mouse knockout library for secreted and transmembrane proteins. *Nature Biotechnol.* **28,** 749–755 (2010).
25. Varoqueaux, F. *et al.* Neuroligins determine synapse maturation and function. *Neuron* **51,** 741–754 (2006).
26. Lesch, K.-P. *et al.* Molecular genetics of adult ADHD: converging evidence from genome-wide association and extended pedigree linkage studies. *J. Neural Transm.* **115,** 1573–1585 (2008).
27. Calboli, F. C. *et al.* A genome-wide association study of neuroticism in a population-based sample. *PLoS ONE* **5,** e11504 (2010).

Supplementary Information is linked to the online version of the paper at www.nature.com/nature.

Acknowledgements We thank R. Winant for mass spectrometry analysis, A. Olson for array tomography assistance, S. Pasca for assistance with quantitative real-time PCR and M. Fabian for technical assistance with cell cultures. This project was funded by a NIDA grant to B.A.B. (R01DA015043). N.J.A. was supported by a Human Frontiers Long Term Fellowship. S.J.S. is supported by grants R01NS0725252 and R01NS077601 from the NIH/NINDS.

Author Contributions N.J.A. and B.A.B. designed the experiments and wrote the manuscript; N.J.A., M.L.B., L.C.F. and C.C. performed and analysed the experiments; and G.X.W. and S.J.S. assisted with data analysis.

Author Information Reprints and permissions information is available at www.nature.com/reprints. The authors declare competing financial interests: details accompany the full-text HTML version of the paper at www.nature.com/nature. Readers are welcome to comment on the online version of this article at www.nature.com/nature. Correspondence and requests for materials should be addressed to N.J.A. (nallen@salk.edu).

©2012 Macmillan Publishers Limited. All rights reserved

METHODS

Purification and culture of RGCs and astrocytes. RGCs were purified by sequential immunopanning to greater than 99% purity from P5–P7 Sprague-Dawley rats (Charles Rivers) and cultured in serum-free medium containing BDNF, CNTF and forskolin on laminin-coated coverslips at 50,000 cells per well, as previously described[1,2]. Cortical astrocytes (MD astrocytes) were prepared as described in ref. 1. In some experiments, astrocytes were prepared by immunopanning (IP astrocytes), as recently described in ref. 5. RGCs were cultured for 7–10 d to allow robust process outgrowth, and were then cultured with astrocyte inserts, ACM, COS-7-conditioned media, thrombospondin, Gpc4 or Gpc6 for an additional 6 d unless stated otherwise.

RGC transfection. RGC transfection with siRNA, along with GFP to mark transfected cells, was carried out using Lipofectamine as described in ref. 28. An OnTarget Plus siRNA pool against GluA1 was obtained from Dharmacon (catalogue number L-097755-01). In companion control experiments, RGCs were transfected with the same amount of either a targeting control (siCyclophilin B) or a non-targeting control (siControl) pool from Dharmacon; results obtained were the same with both.

Mice. *Gpc4*-knockout mice were obtained from Genentech/Lexicon and were generated by homologous recombination targeting exon 3, confirmed by Southern blotting[24]. No Gpc4 was detected by western-blotting-conditioned media prepared from *Gpc4*-knockout astrocytes, demonstrating that no functional protein was being secreted (Supplementary Fig. 5c). Mice were maintained on a mixed genetic background (129/C57bl6/J, crossed three generations onto C57bl6/J), because they seemed less viable when repeatedly crossed onto a pure C57Bl6/J background (N.J.A, unpublished observations). All experiments were carried out using male wild-type and knockout littermates (glypican 4 is on the X chromosome, so experiments compared $Gpc4^{+/y}$ with $Gpc4^{-/y}$). To trace dendrites, *Gpc4*-knockout mice were crossed with Thy1-GFP-M mice obtained from JAX.

Preparation of ACM and siRNA. Cortical astrocytes were cultured in 10-cm plates in serum-containing medium until confluent. Cells were then washed three times with warm DPBS to remove serum, and placed in minimal conditioning medium for 4 d. Conditioning media contained phenol-red-free Neurobasal, glutamine, pyruvate, penicillin and streptomycin. ACM was collected and first centrifuged to pellet dead cells and debris, then placed in centrifugal concentrators (Sartorius) with a size cut-off filter of 5 kDa unless otherwise stated. ACM was concentrated 50-fold. Protein concentration was determined by Bradford assay, and ACM was fed to RGCs at 50–80 $\mu g\,ml^{-1}$. This method produced ACM that induced synaptic activity when fed to RGCs the majority of the time, as long as astrocytes were used soon after isolation and not passaged extensively.

For siRNA experiments, OnTarget Plus siRNA pools against rat glypican 4 (catalogue number, L-098055-01) and glypican 6 (catalogue number, L-106892-01) were obtained from Dharmacon. Following validation, individual siRNAs against glypican 4 (sequence 9) and glypican 6 (sequence 6) were selected and used in all experiments (Supplementary Fig. 6). In companion control experiments, astrocytes were transfected with the same amount of either a targeting control (siCyclophilin B) or a non-targeting control (siControl) pool from Dharmacon; results obtained were the same with both. In rescue experiments, astrocytes were co-transfected with complementary DNA (cDNA) for human glypican 4, which is resistant to the siRNA. Confluent astrocytes were put into single-cell suspension using trypsin, and Amaxa nucleofection was used to introduce siRNA into the astrocytes. Astrocytes were plated into RGC growth medium minus B27 and growth factors for 24 h to recover from the transfection and to allow for knockdown of the RNA and subsequent reduction in secretion of the proteins of interest. Astrocytes were then washed three times with warm DPBS and placed in minimal conditioning medium for 3 d before collection of ACM as outlined above. Comparable results were seen when Lipofectamine, rather than nucleofection, was used to introduce siRNA to astrocytes (data not shown). Knockdown of glypican 4 and glypican 6 was validated by western blotting of ACM for glypican 4 (Proteintech rabbit anti-glypican 4) and glypican 6 (RandD goat anti-glypican 6). RGCs were fed with equal amounts of protein from control and siGlypican4+6 ACM, between 30–40 $\mu g\,ml^{-1}$. ACM was fed to RGCs in a range that was at the low end of the effective dose for control ACM, so that the effect of reducing the levels of glypican 4 and glypican 6 in ACM could be observed. This was necessary owing to incomplete knockdown of glypican 4 and glypican 6 in astrocytes, so the levels present in ACM were reduced rather than eliminated.

Two-dimensional gel electrophoresis. ACM was concentrated as outlined above, loaded onto an IPG strip, pH 3–10, and first separated by isoelectric point followed by separation by mass on an SDS gel following manufacturers' instructions (Biorad). The separated proteins were visualized using silver staining following manufacturers' instructions (Invitrogen).

Column fractionation procedure. ACM was prepared as outlined above and diluted into column loading buffer appropriate for each column. Columns (GE Healthcare) were prepacked and 1 ml in size, and fractionation procedures were carried out at room temperature (18–22 °C) in a tissue culture hood to keep the ACM sterile, using a syringe to apply manual pressure. Ethanolamine, pH 9.5 (20 mM), was used as the buffer in all experiments. Initially each column was tested in isolation and then the columns were combined in series in the following procedure (Supplementary Fig. 3). ACM (3.3 mg), collected from 10×15 cm plates of astrocytes, was diluted in ethanolamine buffer and passed over a heparin column to which the protein of interest did not bind. The unbound fraction was collected and passed over an anion column (Q column), to which the protein of interest did bind. The NaCl (salt) concentration was increased to 0.5 M to remove irrelevant proteins, and then to 2 M to elute proteins of interest. The 0.5–2 M anion column eluate was passed over a hydrophobic interaction column (phenyl (low sub)), to which the protein of interest did bind. The bound proteins were eluted by decreasing the NaCl concentration from 2 M to 0 M. This final eluate contained 32 μg protein (Supplementary Table 1) and was sixfold enriched for functional activity, and was analysed by mass spectrometry. Column fractions were tested by feeding them to RGCs at known protein concentrations, in the presence of thrombospondin to induce structural synapses, followed by electrophysiological recording of total synaptic activity. Before they were fed to RGCs, the column fractions went through a buffer exchange from ethanolamine buffer to Neurobasal, to remove high levels of salt. Pierce Zeba desalt spin columns were used for buffer exchange following manufacturer's instructions.

Mass spectrometry analysis. Both the positive fraction (phenyl column eluate) and the negative fraction (phenyl column unbound fraction) were analysed for comparison. Proteins were analysed in solution, reduced with DTT and alkylated with iodoacetamide, and then digested with trypsin. The liquid peptide mixture was passed over an HPLC column to separate individual peptides, which were then spotted onto a MALDI plate. Individual spots on the MALDI plate were analysed using MS/MS on an Applied Biosystems machine. Peptides were identified using the manufacturer's software and the NCBI database

COS-7 cell overexpression screen. Expression constructs for the majority of the proteins identified from the column fractionation procedure were obtained from Open Biosystems or Origene. The identity of the cDNA was verified by sequencing before use. COS-7 cells were used as a 'negative cell line' in which to express candidates, as COS-7 CM induced little synaptic activity in RGCs (Supplementary Fig. 4). COS-7 cells were transfected with cDNA using Lipofectamine 2000 (Invitrogen) following the manufacturer's instructions. Three hours after transfection, cells were washed three times with warm DPBS and placed into minimal conditioning medium for 3 d, and conditioned media was collected as described for ACM. COS-7 CM was fed to RGCs in the presence of thrombospondin to induce structural synapse formation.

Recombinant proteins and DNA constructs. Full-length cDNA for glypican 4 (rat cDNA from Open Biosystems, clone no. 7124728) or glypican 6 (mouse cDNA from Open Biosystems, clone no. 5008374) with a 6-histidine tag at the amino terminus was cloned into pAPtag5 vector (GenHunter) between the SfiI and XhoI sites. These were expressed in HEK293 cells or astrocytes, which were transfected using Lipofectamine 2000 (Invitrogen) following the manufacturer's instructions. The secreted recombinant protein was then purified from conditioned culture media by Ni-chelating chromatography using Ni-NTA resin (Qiagen) following the manufacturer's instructions. The purity of the protein was assessed by running a sample on an SDS gel and staining with Coomassie blue (Pierce). Protein concentration was assessed by Bradford assay and western blotting for glypican 4 (rabbit anti-glypican 4, Proteintech) or glypican 6 (goat anti-glypican 6, RandD) and the 6-histidine tag (mouse anti-histidine, Abcam), and glypican 4 and glypican 6 were fed to neurons at concentrations between 0.1 and 10 nM. Purified human platelet TSP1 was obtained from Haematologic Technologies and fed to neurons at 5 $\mu g\,ml^{-1}$. For testing candidate glypican 4 interactors, recombinant proteins were purchased and fed at the concentrations indicated in the figure legend.

Glycosylation-deficient glypican 4 was generated by site-directed mutagenesis against the presumed glycosylation attachment sites, as in ref. 29. Mutagenesis was confirmed by DNA sequencing, and by the loss of high-molecular-weight smearing when the purified protein was run on a western blot.

Synapse assay on RGCs. For synapse quantification of RGC cultures, cells were fixed for 7 min with 4% paraformaldehyde (PFA), washed three times in phosphate-buffered saline (PBS) and blocked in 200 μl of a blocking buffer containing 50% normal goat serum and 0.1% Triton X-100 for 30 min. After blocking, coverslips were washed three times in PBS, and 200 μl of primary antibody solution, consisting of mouse anti-bassoon (1:500, Stressgen) and postsynaptic antibody against all isoforms of homer (1:1,000, Chemicon), was added to each coverslip. Coverslips were incubated overnight at 4 °C, washed three times in PBS and incubated with

©2012 Macmillan Publishers Limited. All rights reserved

200 µl of Alexa-conjugated secondary antibodies (Invitrogen) diluted 1:1,000 in antibody buffer. Following incubation for 2 h, coverslips were washed three or four times in PBS and mounted in Vectashield mounting medium with DAPI (Vector Laboratories Inc.) on glass slides (VWR Scientific). Secondary-only controls were routinely performed and revealed no significant background staining.

Mounted coverslips were imaged using a Nikon Eclipse E800 epifluorescence microscope (Nikon). Healthy cells that were at least two cell diameters from their nearest neighbours were identified and selected at random by eye using DAPI fluorescence. Eight-bit digital images of the fluorescence emission at both 594 and 488 nm were recorded for each selected cell using a monochrome charge-coupled-device (CCD) camera and SPOT image capture software (Diagnostic Instruments, Inc.). Set exposures were used for each experiment, and were calculated from the positive control condition (RGC + astrocyte). Merged images were analysed for co-localized puncta by using a custom plug-in (written by Barry Wark and available on request from nallen@salk.edu) for the NIH image-processing package IMAGEJ. In each experiment, 15–30 cells across three coverslips were imaged per condition. Graphs are averages of values obtained from multiple experiments, as detailed in the legend, and are normalized to the 'RGC alone' condition.

GluA1 live surface staining. Rabbit anti-GluA1 (Calbiochem), an antibody recognizing the extracellular region of GluA1, was added to the cell culture medium for 15 min at 37 °C at 5 µg ml^{-1} to label surface AMPA receptors. Cell Tracker Red CMPTX dye (Invitrogen) was added at 0.5 µM during the incubation to label the whole cell. Cells were washed three times with DPBS to remove unbound antibody, fixed for 5 min in 4% PFA (the short fixation time prevents permeabilization of the cell), washed three times with PBS and blocked in 50% goat serum for 30 min at room temperature. After blocking, cells were washed three times with PBS and incubated in goat anti-rabbit Alexa 488 secondary antibody 1:500 for 1 h at room temperature. Coverslips were washed three or four times in PBS and mounted in Vectashield mounting medium with DAPI (Vector Laboratories Inc.) on glass slides (VWR Scientific). Secondary-only controls were routinely performed and revealed no significant background staining. Rabbit polyclonal antibodies against intracellular proteins gave no staining using this method.

Mounted coverslips were imaged using a Nikon Eclipse E800 epifluorescence microscope. Healthy cells that were at least two cell diameters from their nearest neighbours were identified at random using the Cell Tracker Red channel. Eight-bit digital images of the fluorescence emission at both 594 and 488 nm were recorded for each selected cell using a monochrome CCD camera and SPOT image capture software (Diagnostic Instruments, Inc.). Set exposures were used for each experiment, and were calculated from the positive control condition (RGC + astrocyte). The numbers of puncta per cell were analysed using the Integrated Morphometry application in METAMORPH. In each experiment, 15–30 cells across three coverslips were imaged per condition. Graphs are averages of values obtained from multiple experiments, as detailed in the legend, and are normalized to the 'RGC alone' condition.

Surface biotinylation and western blotting. For surface biotinylation of RGCs, cells were plated in 35-mm wells at 250,000 cells per well, and two or three wells were pooled per condition. Biotinylation was performed using a Pierce Cell Surface Protein Isolation Kit with the following modifications. All steps were performed at 4 °C unless otherwise stated. Cells were placed on ice and washed twice with DPBS, and then biotin at 0.25 mg ml^{-1} in DPBS was added for 20 min at 4 °C to label surface proteins. Cells were washed three times with TBS to remove unbound biotin, and lysed in RIPA buffer. RIPA buffer was added to the well for 5 min, and cells were removed by squirting, collected in an Eppendorf tube and rotated for 1 h to solubilize membranes fully. Tubes were then spun at 13,000 r.p.m. (16,000*g*) in an Eppendorf microcentrifuge for 15 min to pellet unsolubilized material, and the supernatant was collected. A sample was collected at this stage to analyse for total protein levels. The remainder of the solubilized proteins were mixed with streptavidin-conjugated beads overnight to isolate the biotinylated proteins. Unbound proteins were removed by centrifugation, and bound biotinylated proteins were collected by incubating the beads in SDS buffer plus DTT for 1 h at room temperature.

Both total RGC lysate proteins and surface RGC proteins were separated by size on 4–15% gradient SDS gels (Biorad) and transferred to PVDF membranes. Membranes were blocked in 5% milk for 1 h at room temperature, washed three times in PBS-Tween and incubated overnight at 4 °C in primary antibodies: mouse anti-β-actin 1:5,000 (Sigma), rabbit anti-NSE 1:1,000 (Polyscience), rabbit anti-GluA1 0.25 µg ml^{-1} (Millipore), rabbit anti-GluA2 0.25 µg ml^{-1} (Millipore), rabbit anti-GluA2/3 2.5 µg ml^{-1} (Millipore) and rabbit anti-GluA4 1:1,000 (Millipore). Horseradish-peroxidase-conjugated anti-mouse and anti-rabbit (1:5,000) were used as secondary antibodies (Millipore), and the detection was performed with an ECL-plus kit from Amersham. Signals were acquired using a QImager CCD system and analysed using the software provided by the manufacturer. Band intensity was normalized to the control (RGC alone) condition in each experiment, and data are presented normalized to RGC alone.

Tissue western blotting. Hippocampi were dissected out in ice-cold PBS, and then each hippocampus was homogenized in 250 µl RIPA buffer containing protease and phosphatase inhibitor cocktails (Pierce). Lysates were solubilized for one hour at 4 °C, spun down to remove unsolubilized material, aliquoted and snap-frozen in liquid nitrogen, and stored at −80 °C until use. Protein concentrations were determined by BCA assay and were typically 5 µg µl^{-1}. For each sample, 5 µg of protein was loaded onto the gel. Blots were probed with antibodies as indicated in the figure legend, and values were normalized to the β-tubulin loading control for each sample.

Electrophysiology in culture. Total synaptic activity and mEPSCs were recorded by whole-cell patch-clamping RGCs at room temperature at a holding potential of −70 mV. The extracellular solution contained 140 mM NaCl, 2.5 mM $CaCl_2$, 2 mM $MgCl_2$, 2.5 mM KCl, 10 mM glucose, 1 mM NaH_2PO_4 and 10 mM HEPES (pH 7.4), plus TTX (1 µM) when mEPSCs were being recorded. Patch pipettes had resistances of 3–5 MΩ and the internal solution contained 120 mM potassium gluconate, 10 mM KCl, 10 mM EGTA and 10 mM HEPES (pH 7.2). We recorded mEPSCs using PCLAMP software for Windows (Axon Instruments), and analysed them using MINI ANALYSIS PROGRAM (SynaptoSoft). Results from at least four separate experiments were pooled for analysis.

Electrophysiology in hippocampal slices. Experiments were carried out on littermate wild-type and *Gpc4*-knockout mice aged P12–P14 and P21–P25, and recordings and analysis were both carried out blind to genotype. A chilled choline-based cutting solution was used for dissection and slicing containing 78.3 mM NaCl, 23 mM $NaHCO_3$, 23 mM glucose, 33.8 mM choline chloride, 2.3 mM KCl, 1.1 mM NaH_2PO_4, 6.4 mM $MgCl_2$ and 0.45 mM $CaCl_2$ (pH 7.4). Parasagittal brain slices of thickness 250 µm containing the hippocampus were cut on a Leica vibratome. Slices were then kept at 31 °C for 25 min in the choline cutting solution and for 30 min in isotonic saline solution (125 mM NaCl, 25 mM $NaHCO_3$, 25 mM glucose, 2.5 mM KCl, 1.25 mM NaH_2PO_4, 2 mM $MgCl_2$ and 2.5 mM $CaCl_2$ (pH 7.4)). Oxygenation (95% O_2, 5% CO_2) was continuously supplied during cutting, recovery and recording. Whole-cell voltage-clamp recordings of hippocampal CA1 pyramidal neurons were performed. Patch pipettes with resistances of 2–4 MΩ were pulled from thick-walled borosilicate glass capillaries and filled with an internal solution containing 130 mM $CsMeSO_3$ (Cs^+ was used instead of K^+ as the main cation to improve voltage uniformity), 4 mM NaCl, 10 mM HEPES, 5 mM EGTA, 0.5 mM $CaCl_2$, 4 mM MgATP, 0.5 mM Na_2GTP, 5 mM QX-314 (to suppress voltage-gated sodium currents), with its pH adjusted to 7.2 using CsOH. Access resistance was monitored throughout the recording and was <20 MΩ.

Recordings were carried out at room temperature in flowing isotonic saline containing 1 µM tetrodotoxin to block voltage-gated sodium channels, the $GABA_A$ receptor antagonist bicuculline (40 µM) and 25 µM D-AP5 to block NMDA receptors to isolate AMPA-mediated mEPSCs. In control experiments all events were eliminated by application of the AMPA receptor antagonist NBQX. We recorded mEPSCs for 5 min and analysed them using MINI ANALYSIS PROGRAM. Cumulative probability plots for the interevent interval and the amplitude of mEPSCs were generated for each cell, and plots from wild-type and knockout cells were averaged to produce the plots shown in the figures. In addition, data were analysed by taking the first 100 events from each cell (these particular events were used to prevent bias from very active cells), pooling them for wild-type and knockout condition, and generating cumulative probability plots from the pooled data. The same results were obtained using both analysis methods.

Analysis of dendrite length. In some recordings, Alexa 488 was included in the patch pipette solution. Slices were fixed for 1 h in 4% PFA on ice following recording, and were washed and mounted in Vectashield for imaging. In parallel experiments, vibratome sections were prepared from wild-type and *Gpc4*-knockout mice that had been crossed with Thy1-GFP-M mice to label sparse subsets of CA1 pyramidal neurons with GFP, and were processed in the same way. Labelled cells were imaged on a Leica confocal microscope. *Z*-stacks were acquired to encompass all of the dendritic area, and the maximum projection of the dendritic area generated. Total dendrite length was analysed using HCA-vision NEURITE ANALYSIS software.

Purification of cortical and hippocampal neurons and astrocytes and qRT-PCR. C57bl6 mouse pups at P7 were used for purifications. Astrocytes were purified using integrin beta 5 immunopanning as described in ref. 5. Neurons were purified using L1 immunopanning as described in ref. 30. RNA was isolated using a Qiagen RNeasy kit following the manufacturer's instructions.

For expression analysis, template cDNA was prepared from 50–200 ng of total RNA by reverse transcription. Immunopanned cells from either cortex or hippocampus were paired, and purity was assessed by enrichment for astrocyte marker (GFAP) and neuron marker (Tuj1). Gene expression was quantified using

©2012 Macmillan Publishers Limited. All rights reserved

quantitative real-time PCR (qRT–PCR) in combination with gene-specific primers and the SYBR GREEN system (Roche). The reactions were performed on an Eppendorf Realplex4 cycler (Eppendorf). All samples were run in duplicates. For each DNA fragment (primer pair), all biological samples, including the input standard curves, were amplified on a common 96-well plate in the same run. The following primer pairs were used: AGGTCGGTGTGAACGGATTTG (Gapdh forward); TGTAGACCATGTAGTTGAGGTCA (Gapdh reverse); TAGACCC CAGCGGCAACTAT (Tuj-1 forward); TTCCAGGTTCCAAGTCCACC (Tuj-1 reverse); GGGGCAAAAGCACCAAAGAAG (GFAP forward); GGGACAACTT GTATTGTGAGCC (GFAP reverse); CTGGAGGGTCCTTTCAACATT (Gpc4 forward); GACATCAGTAACCAGTCGGTC (Gpc4 reverse); TAGTCCTGTAT TGGCAGCCAC (Gpc6 forward); GGCTAATGTCTATAGCAGGGAA (Gpc6 reverse).

Primers efficiency was determined by generating standard curves. For confirmation, quantitative PCR products were sequenced. Values were normalized relative to Gapdh expression. Relative gene expression between paired samples was estimated using the $2^{-\Delta\Delta C_T}$ method.

***In situ* hybridization.** Full-length mouse cDNA for both glypican 4 and glypican 6 was used to generate probes approximately 2 kb in size (Open Biosystems: Gpc4 clone no. 3967797, Gpc6 clone no. 5008374). Digoxigenin-labelled, single-stranded antisense and sense riboprobes were prepared by transcription of the linearized plasmid using either T7 or Sp6 RNA polymerases and a DIG RNA labelling kit (Roche) as per the manufacturer's instructions. *In situ* hybridizations were performed essentially as described in ref. 31 with some modifications for postnatal tissue. Briefly, 10-μm-thick, fresh-frozen sections of mouse brain were air-dried and fixed in 4% paraformaldehyde for 10 min. After washing with PBS three times for 10 min each time, sections were acetylated by incubation in 0.1 M triethanolamine HCl and 0.25% acetic anhydride for 10 min. After washing with PBS three times for 5 min each time, hybridization was performed with probes at concentrations of 200–500 ng ml^{-1} in a hybridization solution (50% formamide, ×5 SSC, ×5 Denhardt's solution, 250 μg ml^{-1} baker's yeast RNA and 100 μg ml^{-1} salmon sperm DNA) at 72 °C for 16 h. After hybridization, slides were washed once in ×0.2 SSC at 72 °C for 60 min, once in ×0.2 SSC at room temperature for 5 min and once in buffer B1 (0.1 M Tris HCl (pH 7.5) and 150 mM NaCl) for 5 min, incubated in B1 with 10% normal goat serum for 1 h, and then incubated in B1 with 1% normal goat serum and 1:1000 anti-digoxygenin alkaline-phosphatase conjugated antibody (Roche) overnight at 4 °C. Slides were then washed in B1 three times for 5 min each time, equilibrated in buffer B3 (0.1 M Tris HCl (pH 9.5), 100 mM NaCl and 50 mM $MgCl_2$) four times for 15 min each time and then developed in B3 with 0.24 mg ml^{-1} levamisole, 0.375 μl ml^{-1} NBT and 3.5 μl ml^{-1} BCIP (Roche) until a colour precipitate was visible. The reaction was stopped by washing once in TBST and four times in water, and slides were mounted with coverslips using Glycergel mounting medium (Dako).

For GFAP immunostaining, anti-mouse GFAP antibody (Sigma) at 1:1000 was added with anti-digoxygenin antibody overnight at 4 °C. After washing in B1 three times for 5 min each time, anti-mouse Fc horseradish-peroxidase-conjugated antibody was added in 1% goat serum in B1 (1:500) for 2 h at room temperature before alkaline phosphatase was developed as above. Following washes in water, horseradish peroxidase was developed using DAB reagent (Vector Labs) for 8 min. Slides were washed six times in water and mounted with coverslips using Glycergel mounting medium.

Array tomography. Array tomography was carried out as described in ref. 32. Hippocampal slices from P12 *Gpc4*-knockout and wild-type littermate controls were prepared in the same way as for electrophysiological analysis (300-μm vibratome sections of live tissue), fixed with 4% PFA overnight at 4 °C, and then dehydrated and embedded in LRWhite resin using the benchtop protocol. Ribbons of 30–35 serial ultrathin sections (70–100 nm) were cut on an ultramicrotome (Leica), mounted on subbed glass coverslips and immunostained using antibodies against VGLUT1 (guinea pig, Millipore), GluA1 (rabbit, Abcam) and pan-MAGUK (mouse, NeuroMabs). Antibody binding was visualized using Alexa-488-, Alexa-594- and Alexa-647-labelled goat secondary antibodies (Invitrogen). Sections were mounted using SlowFade Gold antifade with DAPI (Invitrogen). Images were collected on a Zeiss Axiovert 200M fluorescence microscope with an AxioCam HRm CCD camera, using a Zeiss ×63/1.4 NA Plan Apochromat objective. The hippocampal area CA1 stratum radiatum was imaged, to analyse synapses proximal to the pyramidal neuron cell body.

Tissue volumes were reconstructed and aligned using IMAGEJ (NIH) and the multistackreg plug-in (Brad Busse), and then cropped to include CA1 stratum radiatum so that the same volume was analysed across animals. Image deconvolution was carried out using a custom function in MATLAB (Gordon Wang). Individual puncta were identified for each channel, and then the number of MAGUK + GluA1 co-localized puncta associated with a VGLUT1 puncta was quantified using a separate custom function in MATLAB (Gordon Wang). Puncta numbers were normalized to wild-type values.

Data analysis and presentation. All graphs represent average data with s.e.m. error bars. Statistical analysis was either by Student's *t*-test when only two groups were being compared, or by one-way analysis of variance when three or more groups were compared.

28. Eroglu, C. *et al.* Gabapentin receptor α2δ-1 is a neuronal thrombospondin receptor responsible for excitatory CNS synaptogenesis. *Cell* **139,** 380–392 (2009).
29. Williams, E. H. *et al.* Dally-like core protein and its mammalian homologues mediate stimulatory and inhibitory effects on Hedgehog signal response. *Proc. Natl Acad. Sci. USA* **107,** 5869–5874 (2010).
30. Steinmetz, C. C., Buard, I., Claudepierre, T., Nagler, K. & Pfrieger, F. W. Regional variations in the glial influence on synapse development in the mouse CNS. *J. Physiol. (Lond.)* **577,** 249–261 (2006).
31. Schaeren-Wiemers, N& Gerfin-Moser, A. A single protocol to detect transcripts of various types and expression levels in neural tissue and cultured cells: in situ hybridization using digoxigenin-labelled cRNA probes. *Histochem. Cell Biol.* **100,** 431–440 (1993).
32. Micheva, K. D. & Smith, S. J. Array tomography: a new tool for imaging the molecular architecture and ultrastructure of neural circuits. *Neuron* **55,** 25–36 (2007).

©2012 Macmillan Publishers Limited. All rights reserved